MULTIPLY STRIPPED ION GENERATION IN THE METAL VAPOR VACUUM ARC*

I. G. Brown, B. Feinberg and J. E. Galvin

Lawrence Berkeley Laboratory
University of California
Berkeley, CA   94720

September 1987

ABSTRACT

We consider the charge state distribution of ions produced in the metal vapor vacuum arc plasma discharge. A new kind of high current metal ion source in which the ion beam is extracted from a metal vapor vacuum arc plasma has been used to obtain the spectra of multiply charged ions produced within the cathode spots. The cathode materials used and the species reported on here are: C, Mg, Al, Si, Ti, Cr, Fe, Co, Ni, Cu, Zn, Zr, Nb, Mo, Rh, Pd, Ag, In, Sn, Gd, Ho, Ta, W, Pt, Au, Pb, Th, and U; the arc current was 200 A for all measurements. Charge state spectra were measured using a time-of-flight method. The arc voltage was also measured. In this paper we report on the measured charge state distributions and arc voltages and compare the distributions with the predictions of a theory in which ionization occurs in the cathode spots via stepwise ionization by electron impact.

I. INTRODUCTION

The metal vapor vacuum arc is a plasma discharge that occurs between conducting electrodes in vacuum. As the arc proceeds, material is evolved from the electrodes, mostly from the cathode so long as the arc current is not too high, and a dense metal plasma is created. The fundamental phenomenon which drives the vacuum arc is that of cathode spot formation - minute regions of intense current concentration which reside on the surface of the cathode and at which the solid cathode material is vaporized, ionized, and injected into the interelectrode arc region. The current density at the cathode spots is of order 10^6 A/cm^2 over a spot size of order microns. A typical vacuum arc discharge might consist of from one to many dozens of such spots. It is within the intense fireball of the cathode spot that the plasma constituents of the arc are formed - the parameters of the arc are in large part determined by the plasma physics of the spots. Thus an understanding of the cathode spot plasma is essential to any attempt to use or control the arc as a plasma device.

The study of the metal vapor vacuum arc discharge, also called the vacuum arc or metal vapor arc, had its origin in the high power switching field. One of the earliest publications in the field is that of Sorensen and Mendenhall in 1926[1]; early work was severely impeded by the rudimentary vacuum techniques of the era. An historical survey of the field, pre-1960s, has been given by Cobine[2]. More recently a very complete review of the entire field of metal vapor arc discharges has been given by Lafferty[3] and a review of cathode spot behavior has been given by Lyubimov and Rakhovskii[4].

The production of ions in the metal vapor vacuum arc plasma has been investigated by a number of authors over at least the last two decades[5-20]. One of the earliest attempts to incorporate this kind of arc as the plasma formation mechanism within an ion source was the work done as part of the Manhattan Project in World War II[21]; the source suffered from several drawbacks and this work was abandoned. Revutskii et al[22], in 1968, described a cylindrically symmetric arc geometry employing ion extraction through a hole in the cathode (as opposed to through the anode, as in our work, to be described), and their work appears not to have been pursued. More recently, sources of this kind have been described by Adler and Picraux[23], and by Humphries and coworkers[24-27].

We have developed an ion source in which the metal vapor vacuum arc is used as the method of plasma production and from which high quality, high current beams of metal ions can be extracted[28-33]. We have called this source the MEVVA ion source, as an acronym for the mechanism employed. With this source we have produced beams at voltages up to 100 kV and with ion currents up to 1 Ampere. The source works well with a wide range of ion species, spanning the periodic table from lithium to uranium. In general, for elements not too low on the periodic table, the ions produced are multiply ionized.

The average charge state is generally higher for higher Z elements and for materials with a high boiling point, and to a lesser extent for higher arc current. For example, a tungsten beam typically is composed of species with charge state from $Q = 1$ to 5, a chromium beam has charge states $Q = 1$, 2 and 3, and a lithium beam consists of the singly ionized $Q = 1$ species only. For almost all applications of the source, there is considerable advantage to a beam with ions stripped maximally. Hence our interest in understanding the physics of the MEVVA charge state distribution and in trying to achieve upwards control over the distribution.

Measurements of the charge state distribution of ions generated by the vacuum arc have previously been reported by several workers[5,6,8] and it is well recognized that the distributions in general contain a high fraction of multiply stripped species. Theoretical understanding of the cathode spot plasma is, however, very incomplete.

II. EXPERIMENTAL SET-UP

The MEVVA ion source has been described elsewhere[28-33]. Briefly, in this source we make use of the intense plume of highly ionized metal plasma that is created at the cathode spots of a metal vapor vacuum arc discharge to provide the "plasma feedstock" from which the ion beam is extracted. The quasi-neutral plasma plumes away from the cathode toward the anode and persists for the duration of the arc current drive. The anode of the discharge is located on axis with respect to the cylindrical cathode and has a central hole through which a part of the plasma plume streams; it is this component of the plasma that forms the medium from which the ions are extracted.

The plasma plume drifts through the post-anode region to the set of grids that comprise the extractor - a three grid, accel-decel, multi-aperture design. A small axial magnetic field of up to about 100 gauss produced by a simple coil surrounding the arc region serves to help duct the plasma plume in the forward direction, but this is not essential to the source operation.

A schematic of an embodiment of the concept with which we've done much of our ion source developmental work is shown in Figure 1; the various components and features referred to above can be seen. For the work described here, we have used the MEVVA IV ion source, a version in which 16 separate cathodes are mounted in a single cathode assembly, allowing the operational cathode to be changed simply by rotating a knob so as to position the desired cathode in line with the anode and extractor of the device. Thus many different cathode materials can be compared in a relatively short experimental run and with confidence in maintaining the same experimental conditions. A photograph of the MEVVA IV source is shown in Figure 2.

The arc is driven by a simple pulse line. The line is a 6-section LC network of impedance 1 Ohm and pulse length 250 microseconds, with a modified Gibbs section on the front end to provide a fast rise to the pulse. The line is charged to a voltage of up to several hundred volts with a small, isolated, dc power supply. A high voltage pulse applied to a trigger electrode initiates a surface spark discharge between the trigger electrode and the cathode, which in turn causes the main anode-cathode circuit to close due to the spark plasma, and the vacuum arc proceeds. Typically the source is operated at a repetition rate of several pulses per second, up to a maximum of near 100 pulses per second for short pulse length and low average power; we are presently increasing the duty cycle at which the source will run. For all the measurements reported on here the arc current was 200 A.

The source is operated on a test-stand equipped with various diagnostics to monitor the source performance and the parameters of the extracted beam. Base pressure is in the low 10^{-6} Torr range. The arc current is routinely monitored; the arc voltage (anode-cathode drop) is measured only when beam is not extracted, since during extraction the arc circuit is biased to the full extraction potential of up to 100 kV; for this series of measurements the extraction voltage was 60 kV. In the work described here the small magnet

coil surrounding the arc was not energized; the major effect of this field is to increase the efficiency with which the arc plasma is transported to the extractor[33], but this is not a concern for the present work. Beam current is measured by a magnetically suppressed Faraday cup, and we have cross-checked these measurements with those obtained using several different designs of beam calorimeters. Beam divergence and emittance were measured with a 16-collector beam profile monitor[34,35] and with a "pepper pot" device[36]. We find that a beam current of several hundred milliamperes into a half-angle divergence of from 1° to 3°, or an emittance of < 0.05 π cm mrad (normalized), can be produced routinely. Both the extracted beam current and the emittance of the extracted beam are sensitive functions of the geometry of the extractor, the extraction voltage, the plasma density, the ion mass, and the magnetic field strength; the beam current is not a parameter of any relevance to the charge state distribution, and is not considered here.

The ion source, its operation, and the supporting facilities have been fully described in references 28 – 33, to which the reader is referred for more detail.

The charge state distribution (CSD) of the extracted ion beam has been measured using a time-of-flight (TOF) diagnostic. In this device a set of deflection plates is located in the beam path and biased so as to deflect the beam aside except for a short pulse of about 0.2 μs in length that is gated from the middle (plateau) part of the beam pulse; in this way a short sample of the beam is obtained. This short pulse is allowed to drift down a 1.95 m long region, during which drift time the different charge-to-mass (Q/A) components of the beam separate out, since they have been accelerated through the same potential drop in the ion source extractor and thus have flight times proportional to $(Q/A)^{-\frac{1}{2}}$. A detector, a well-shielded Faraday cup with magnetic suppression of secondary electrons, at the end of the drift chamber measures the arrival time of the different Q/A components of the beam. The detector is prevented from viewing the intense visible light and UV generated by the vacuum arc by blocking the direct path with a metal plate; the beam is steered onto the detector by the deflection plates. The detector measures the electrical current in the different charge states and provides a good measurement of the CSD of the extracted ion beam. The measured flight times for the various charge states are well fitted by the calculated values, usually to better than the measurement uncertainty of about

1%. We did no special preparation of any of the cathodes; the cathode surface was simply "as machined". After a clean-up period of typically less than 100 firings of the ion source the measured spectra were generally quite clean, with minimal impurity contamination visible. For one case (uranium), we vacuum baked the cathode at 600°C for 24 hours and compared the spectrum obtained using this well-outgassed cathode with that obtained using an unbaked cathode; after a short clean-up period, the spectra were identical. The time-of-flight system has been described in more detail in reference 37.

A schematic of the experimental configuration is shown in Figure 3.

III. THEORETICAL MODEL

The term "cathode spot" is used somewhat loosely in the literature to refer to that region on the cathode surface into which current is concentrated in the vacuum arc plasma discharge. In general many cathode spots will participate simultaneously in the arc; as the arc current is increased, more spots form. By processes which are not at all well understood and about which there is still much discussion, it is within the cathode spots that material is removed from the solid surface and ejected away from the cathode in the plasma state. For distances sufficiently close to the cathode surface, the plasma is of high density and collisional, and the parameters of the plasma are determined in this collisional zone. It is this region to which we restrict our attention in the following. Thus, inherent in the simplistic approach that we are adopting here is an averaging over the collisional region. We want to stress that we do not consider this approach to be the ultimate in theoretical sophistication, but it is an approach that is amenable to analysis, and to which further layers of theory can later be added if warranted. We do not consider here the origin of the cathode spots nor the mechanism that maintains them, but only the spatially averaged plasma parameters that are implied by the measured charge state distributions.

In the model, ions are created within the cathode spot plasma by ionization from the neutral state by electron impact. The plasma ions may be further stripped by a number of different processes, of which the most important is stepwise ionization by successive electron impact[38]. Multiple ionization - the removal of several electrons in a single collision - has been examined experimentally and theoretically by Mueller[39,40]. While

multiple ionization is likely to be significant at these electron temperatures for high Z (Z $\gtrsim$ 60), it has not been included because of the lack of a good general model. In addition, ionization of excited states, which is also likely to be significant at these high densities, has been omitted in this simple model, as has ion-ion charge transfer. The time history of the charge state distribution is determined by the electron energy, E_e, and the product $n_e\tau_i$ of electron density n_e and ion residence time within the stripping region, τ_i. Thus the plasma electrons must be sufficiently energetic to remove the bound electrons by collisions, and the plasma electron density and ion residence time within the plasma must be sufficiently great to allow the stripping to proceed. Calculations of the parameters necessary to achieve given charge states for a variety of elements have been carried out by a number of authors.[41-43]

The computer code developed here integrates a set of coupled rate equations of the form

$$
\begin{aligned}
\frac{dn_i}{dt} = \quad & n_{i-1}n_e\langle\sigma_{i-1,i}v\rangle \quad - \quad n_in_e\langle\sigma_{i,i+1}v\rangle \\
& - \quad n_in_eR_{i,i-1} \quad + \quad n_{i+1}n_eR_{i+1,i} \\
& - \quad n_in_0(C_{i,i-1} \quad + \quad C_{i,i-2}) \\
& + \quad n_{i+1}n_0C_{i+1,i} \quad + \quad n_{i+2}n_0C_{i+2,i}
\end{aligned}
\tag{1}
$$

where n_i is the density of ions of charge state i, n_e is the electron density and n_0 is the background neutral density. $\sigma_{i,i+1}$ is the cross section for ionization from charge state i to charge state $i+1$ by impact with electrons of velocity v, and the average $\langle\sigma v\rangle$ is taken over the distribution of electron velocities. The cross sections, binding energies and ionization potentials are as given by Lotz[44-46] and Carlson et al[47,48]. The recombination rates $R_{i,i-1}$ are given by McWhirter[49], and the ion-neutral charge exchange rates $C_{j,j-1}$, $C_{j,j-2}$ are given by Mueller and Salzborn[50].

The initial conditions (parameters input into the calculation from which the computed plasma charge state distribution evolves) include a neutral density that decreases with time, since the neutrals decrease in number as they traverse the spot plasma and are ionized. The electron density is represented as a cylinder with a Gaussian radial distribution, and the neutral density input from the cathode is also given a Gaussian radial distribution.

This kind of calculation has been used to predict the charge state distributions of ions produced in EBIS (Electron Beam Ion Source) devices. In the EBIS, ions are confined within the electrostatic well of an intense, energetic electron beam and they are stripped to high charge state by collisions with the beam electrons; these sources have been developed at a number of laboratories[51,57]. EBIS data provide a good reference with which to compare the predictions of a stripping theory, because of the well-defined electron energy, electron density, and ion residence time. Such a comparison has been made by Donets[51,58]. For the present work we have compared the predictions of the computer program developed here against the same EBIS data as a check on the program. The comparison was good.

Charge state distributions have been calculated for the cathode materials with which the MEVVA ion source has been run. The computer program provides a graph of the ion fraction in each charge state as a function of time, given the electron density and velocity distribution and other initial conditions. The results of a typical calculation are shown in Figure 4, where the time evolution of the charge state distribution for titanium is shown. A "time slice" of the charge state distribution can then be chosen for comparison with the experimental data. In this comparison the confinement time τ_i of the theoretical treatment is equivalent to the mean ion residence time within the cathode spot, a lower limit to which is the ion flight time across the spot dimension.

IV. RESULTS

The TOF spectra measured here are shown in Figure 5. These were all taken for the same arc current, I_{arc} = 200 A, and for a beam extraction voltage V_{ext} = 60 kV; the oscillogram sweep speed is 1 μs/cm. These spectra were obtained as ion current collected by a Faraday cup, and the amplitudes of the charge state peaks in the oscillograms are proportional to electrical current; the electrical current is greater than particle current by the charge state Q, $I_{elec} = QI_{part}$. In order to obtain spectral data that would be visually intercomparable, the oscilloscope gain was adjusted for each cathode material, and the vertical current scale in the Figure 5 oscillograms is not the same for different materials; none-the-less, the current scale is always within a factor of several of 100 μA/cm. The CSD data shown in Figure 5 is summarized in Table I.

Figure 6 shows two examples of TOF spectra obtained for the case when the cathode material is a conducting compound rather than a metallic element. The spectra shown are for titanium carbide and lead sulfide; (these data were taken under different conditions of arc current and extraction voltage). The results are significant in several ways. Firstly, it is evident that beams containing non-conducting species can be produced; cathode spots form on the surface of the conducting cathode and the non-conducting component of the molecule participates in the plasma as well as the conducting. Secondly, the ionization states of the elemental constituents of the "compound discharge" can be different from those produced in the "elemental discharge". Thus C^{2+} is evident in the TiC spectrum, but we have never seen C^{2+} from a carbon cathode - only the singly ionized C^+.

The arc voltage was also measured. Using a differential probe technique so as to minimize errors due to ground loop and pick-up signals, the voltage across the anode-cathode terminals of the ion source was monitored. An oscillogram of arc voltage and arc current for the case of a copper cathode is shown in Figure 7. The voltage was measured in the flat portion of the trace, about half way into the current waveform, as was also the TOF spectrum. The arc voltage measurements are also listed in Table I. In making these measurements we made many checks, cross-checks and calibrations, and the uncertainty in all cases is no greater than ±1.5 V. We have omitted C and Si measurements, as the resistivity of the cathode material itself gives rise to unreliable voltage data.

V. DISCUSSION

We compare the results obtained here to those of other workers. Results have been presented in the literature of both charge state distribution and arc voltage measurements for a number of cathode materials.

In measuring the current of multiply charged ions one must distinguish between electrical current and particle current. As mentioned above, for a beam of ions of charge state Q, the electrical current is greater than the particle current by the factor Q: $I_{elec} = QI_{part}$. This distinction is of some importance, and seems not to have always been made clear in the literature. For example, if the current measured is electrical current, then the fraction of ions in the highest charge states of the distribution

(particle current) can be lower by as much as a factor of two than would at first sight seem to be implied from the measured distribution (electrical current). Here, the detector is a Faraday cup and the signal measured is electrical current. Depending on the application or concern, one might be interested in either the electrical current or the particle current. However, the particle current is a more fundamental parameter, and in Table I we list the charge state fractions both of electrical current and of particle current (renormalized). The mean charge states, $\bar{Q} = \sum fQ/\sum f$, where f is the charge state fraction, are also listed for both of these formats, $\bar{Q}_e$ and $\bar{Q}_p$.

A comparison of charge state distribution data obtained here with such data as are available from a number of other sources is shown in Table II. In all cases (both the results presented here and those of other workers), the CSD is that of the ions generated by the cathode spots but measured at a distance from the cathode. Arc current was not greatly different between the various experiments, and in any case the CSD changes only minimally with arc current. In Table II we have shown the distributions measured here expressed both in terms of electrical current (I_{el}) and particle current (I_{part}), from Table I. It is not clear if the references used for comparison have quoted electrical current or particle current. Depending on the detector used for measurement of the charge state spectrum, the signal can be I_{el} or I_{part} or somewhere in between; see reference 37 for an experimental investigation of this concern. In any case, the differences between our results and those of other workers, for those cases for which comparisons can be made, are not great. Our results cover a wider range of cathode species and greatly extend the data.

A similar comparison of our arc voltage measurements with the measurements of other workers is shown in Table III. Again, the comparison is good, with the results presented here being considerably more extensive.

In an attempt to provide a phenomenological method for predicting the CSD, we have looked at the measured mean charge state, $\bar{Q}$, for the various cathode materials as a function of a number of parameters, including atomic number Z, melting point, boiling point, and heat of fusion. There is a trend in the data when so plotted for all of these cases, but the fit is best when plotted against the boiling point temperature, I_{BP}. In Figure 8 the mean charge

state, refered to particle current, $\overline{Q}_p$, is plotted as a function of boiling point (°K) for all the elemental cathode materials investigated here. The straight line shown has been obtained through a linear regression (least squares best fit) to the data points, excluding the four elements which show the greatest departure from the trend - C, Mg, In, and Pt. The line is given by

$$\overline{Q}_p = 0.38(T_{BP}/1000) + 0.6. \qquad (2)$$

This expression provides a reasonably good fit to the data, apart from the four materials excluded, with a correlation coefficient of 0.84. It might be useful as a predictor, even though completely phenomenological.

The computer program described in Section III has been used to fit the measured CSDs. The electron energy distribution is taken as Maxwellian. The initial particle population is allowed to evolve without input of fresh neutrals; the lower charge states "burn out" as they are stripped to higher Q values, and are not replaced. It should be noted that for the parameters of interest, recombination plays a negligible role. Charge exchange with background neutrals is negligible also, since the source operates at very low pressures once the cathode surface is degassed by the initial shots.

An example of how the calculations can provide a fit to the measured spectra is shown. Figure 9 shows the measured and calculated CSDs for titanium. The experimental data have been taken directly from Figure 5, and the calculated values from Figure 4. (The charge state fractions shown in Figure 4 are particle current; for comparison with the experimental data in Figure 9, they have been multiplied by Q, $I_e = QI_p$). Parameters for the calculation, which were optimized for titanium, were: T_e = 4.6 eV and $j_e\tau_i$ = 8 x 10^{17} electrons/cm^2. For a cathode spot current density of 10 MA/cm^2 then τ_i = 13 nsec, in which time a titanium ion of energy 4.6 eV will traverse a distance of 56 microns, in the absence of collisions. These values for current density and spot size are in order-of-magnitude agreement with what is conventionally considered to be typical of cathode spots. The electron temperature required for the fit, 4.6 eV, is also consistent with what is considered typical.[59-62]

The program is used to fit the data in the following manner. We assume that the electrons leave the cathode with an energy proportional to the arc voltage, and that they lose energy in exciting and ionizing ions and through collisions with the electrons produced by ionization. This results in an electron temperature approximately proportional to the arc voltage, for all elements. Another assumption is that the electron density is constant for all cathode materials. Finally, we assume the ions move with a velocity proportional to the acoustic velocity, $c_s = (kT_e/M_i)^{\frac{1}{2}}$, which results in a residence time in the ionizing region inversely proportional to the acoustic velocity. We calculate the average charge state for each element as a function of time, using an electron temperature proportional to the measured arc voltage. Comparing these results with the experimental data results in a residence time for each element. By the above assumptions the residence time times the acoustic velocity must be a constant, so an optimum value for this constant is calculated. We then use this constant to calculate the average charge state for each cathode material. This procedure is then repeated using a different fraction of the arc voltage for the electron temperature, and an optimum solution found. Figure 10 shows the measured and calculated mean charge states plotted as a function of Z. The fit to the data is quite reasonable. The electron temperature used is the arc voltage divided by 4.5, and $j_e \tau_i (T_e/A)^{\frac{1}{2}} = 1.6 \times 10^{17}$ (electrons/cm^2)(eV/amu)$^{\frac{1}{2}}$. For the range of cathode materials covered here the electron temperature in this model is thus 3 - 6 eV.

We conclude that the ionization model presented here – which is similar to models used to provide descriptions of the charge state evolution in other multiply-ionized plasmas such as the EBIS[51,52,58] and ECR[63,64] ion sources – provides a reasonable description of the cathode spot plasma. Here we have included only stepwise ionization (removal of electrons one at a time) and have neglected multiple ionization (removal of several electrons in a single collision), and we have also neglected ionization from excited states; both of these effects could be significant here. It might be fruitful to develop the model further to include these effects. The plasma physics of the cathode spot is poorly understood, and further studies of this kind might shed some light.

VI. CONCLUSION

Measurements have been made of the charge state distribution of the ions produced by the metal vapor vacuum arc for a wide range of cathode materials. In general, multiply charged ions are produced, and the mean charge state, $\bar{Q}$, increases with the boiling point of the cathode material. An approximate phenomenological fit to the data is provided by the formula $\bar{Q}_p = 0.38(T_{BP}/1000) + 0.6$, where $\bar{Q}_p$ is the mean charge state in terms of particle current and T_{BP} is the boiling point temperature in °K. The charge state distribution measurements presented here are generally consistent with the results of other workers, as reported in the literature, as are also the arc voltage measurements. The range of materials reported on here is considerably more extensive than has been previously available.

A theoretical model has also been presented which provides a reasonable fit to the experimental results. In this model all the ionization is assumed to take place within the cathode spot plasma, and multiple stripping to higher ionization states is considered to occur by stepwise ionization by successive electron impact. The plasma parameters predicted by the model are consistent with what has been considered typical of the cathode spot plasma.

These results are important fundamentally because they add to the pool of knowledge about cathode spot behavior, a plasma phenomenon still far from understood. The MEVVA ion source has demonstrated itself as being a suitable tool for investigation of the physics of metal vapor vacuum arcs. Finally, the data provide the MEVVA ion source user with practical information on source performance.

ACKNOWLEDGMENTS

REFERENCES

1. R. W. Sorensen and H. E. Mendenhall, Trans. AIEE, Pt. III, 45, 1102 (1926).

2. J. D. Cobine, Elect. Eng. 81. 13 (1962).

3. J. M. Lafferty, editor, "Vacuum Arcs – Theory and Application", John Wiley and Sons, New York, 1980.

4. G. A. Lyubimov and V. I. Rakhovskii, Sov. Phys. Usp. 21(8), 693 (1978).

5. A. A. Plyutto, V. N. Ryzhkov and A. T. Kapin, Sov. Phys. JETP 20, 328 (1965).

6. W. D. Davis and H. C. Miller, J. Appl. Phys. 40, 2212 (1969).

7. C. W. Kimblin, J. Appl. Phys. 44, 3074 (1973).

8. V. M. Lunev, V. G. Padalka and V. M. Khoroshikh, Sov. Phys. Tech. Phys. 22(7), 858 (1977).

9. M. S. Agarwal and R. Holmes, J. Phys. D: Appl. Phys. 17, 757 (1984).

10. J. E. Daalder, Physica 104C, 91 (1981).

11. J. E. Daalder, J. Phys. D: Appl. Phys. 8, 130 (1975).

12. C. W. Kimblin, Proc. IEEE 59, 546 (1971).

13. A. S. Gilmour, Jr., and D. L. Lockwood, Proc. IEEE 60, 977 (1972).

14. H. C. Miller, J. Appl. Phys. 52, 4523 (1981).

15. J. W. Robinson and M. Ham, IEEE Trans. Plasma Sci. PS-3, 222 (1975).

16. J. E. Daalder J. Phys. D: Appl. Phys. 9, 2379 (1976).

17. E. Hantzsche, Proceedings of the 13th International Conference on Phenomena in Ionized Gases (Physical Society, GDR, Berlin, 1977), Vol. 3, p. 121.

18. D. T. Tuma, C. L. Chen and D. K. Davies, J. Appl. Phys. 49, 3821 (1978).

19. IEEE Trans. Plasma Sci. PS-11, No. 3 (1983). Special issue on vacuum discharge plasmas.

20. IEEE Trans. Plasma Sci. PS-13, No. 5 (1985). Special issue on vacuum discharge plasmas.

21. R. K. Wakerling and A. Guthrie, editors, "Electromagnetic Separation of Isotopes in Commercial Quantities", (McGraw Hill, New York, 1951), p. 324.

22. E. I. Revutskii, G. M. Skoromnyi, Yu. F. Kulygin and I. I. Goncharenko, in Proceedings of the Soviet Conference on Charged Particle Accelerators, Moscow, 9-16 October 1968, edited by A. A. Vasilev, Vol. 1, p. 447. (published for the US AEC and NSF, Washington, DC, by the Israel Program for Scientific Translations).

23. R. J. Adler and S. T. Picraux, Nucl. Instrum. and Methods B6, 123 (1985).

24. S. Humphries, Jr., M. Savage and D. M. Woodall, Appl. Phys. Lett. $\underline{47}$, 468 (1985).

25. C. Burkhart, S. Coffey, G. Cooper, S. Humphries, Jr., L. K. Len, A. D. Logan, M. Savage and D. M. Woodall, Nucl. Instrum. and Methods $\underline{B10}$, 792 (1985).

26. S. Humphries, Jr., C. Burkart, S. Coffey, G. Cooper, L. K. Len, M. Savage, D. M. Woodall, H. Rutkowski, H. Oona and R. Shurter, J. Appl. Phys. $\underline{59}$, 1790 (1986).

27. L. K. Len, C. Burkart, G. W. Cooper, S. Humphries, Jr., M. Savage and D. M. Woodall, IEEE Trans. Plasma Sci. $\underline{PS-14}$, 256 (1986).

28. I. G. Brown, J. E. Galvin and R. A. MacGill, Appl. Phys. Lett. $\underline{47}$, 358 (1985).

29. I. G. Brown, IEEE Trans. Nucl. Sci. $\underline{NS-32}$, 1723 (1985).

30. I. G. Brown, J. E. Galvin, B. F. Gavin and R. A. MacGill, Rev. Sci. Instrum. $\underline{57}$, 1069 (1986).

31. I. G. Brown, J. E. Galvin, R. Keller, P. Spaedtke, R. W. Mueller and J. Bolle, Nucl. Instrum. and Methods $\underline{A245,}$ 217 (1986).

32. I. G. Brown, J. E. Galvin, R. A. MacGill and R. T. Wright, 1987 Particle Accelerator Conference, Washington, D.C., March 1987.

33. I. G. Brown IEEE Trans. Plasma Sci. (to be published).

34. J. E. Galvin and I. G. Brown, Rev. Sci. Instr. $\underline{55}$, 1866 (1984).

35. J. E. Galvin and I. G. Brown, Rev. Sci. Instr. $\underline{56}$, 1972 (1985).

36. R. Keller, GSI 1980 Annual Report, GSI Report 81-2, p. 263.

37. I. G. Brown, J. E. Galvin, R. A. MacGill and R. T. Wright, Rev. Sci. Instrum. $\underline{58}$, 1589 (1987).

38. B. L. Schram, Physica $\underline{32}$, 197 (1966).

39. A. Mueller, Physics Letters $\underline{113A}$, 415 (1986).

40. A. Mueller, C. Achenbach, E. Salzborn and R. Becker, J. Phys. B, $\underline{17}$, 1427 (1984).

41. H. Winter and B. H. Wolf, in Proceedings of the Second Symposium on Ion Sources and Formation of Ion Beams, Berkeley, California, October 1974; Lawrence Berkeley Laboratory Report LBL-3399, paper V-1.

42. H. Winter, in "Experimental Methods in Heavy Ion Physics", Lecture Notes in Physics Series, edited by K. Bethge (Springer, Berlin, 1978), p. 14.

43. Laboratoire National Saturne, Report SFEC 1 10 - Cryebis II, Center for Nuclear Studies, Saclay, France, 1981.

44. W. Lotz, Z. Phys. $\underline{216}$, 241 (1968).

45. W. Lotz, J. Opt. Soc. Am. 57, 873 (1967).

46. W. Lotz, J. Opt. Soc. Am. 58, 915 (1968).

47. T. A. Carlson, C. W. Nestor, Jr., N. Wasserman and J. D. McDowell, Atomic Data 2, 63 (1970).

48. T. A. Carlson and B. P. Pullen, Oak Ridge National Laboratory Report, ORNL-4393 (1969).

49. R. W. P. McWhirter, in "Plasma Diagnostic Techniques", edited by R. H. Huddlestone and S. L. Leonard (Academic Press, New York, 1965), p. 210.

50. A. Mueller and E. Salzborn, Phys. Lett. 62A, 391 (1977).

51. E. D. Donets, IEEE Trans. Nucl. Sci. NS-23, 897 (1976).

52. J. Arianer and C. Goldstein, IEEE Trans. Nucl. Sci. NS-23, 979 (1976).

53. R. Becker and H. Klein, IEEE Trans. Nucl. Sci. NS-23, 1017 (1976).

54. R. W. Hamm, Los Alamos Scientific Laboratory report LA-7077-T (1977).

55. Proceedings of the Workshop on Electron Beam Ion Sources and Related Topics, June 15-16, 1977, Darmstadt, Germany, edited by B. H. Wolf and H. Klein, (GSI, Darmstadt).

56. I. G. Brown and B. Feinberg, Nucl. Instr. and Meth. 220, 251 (1984).

57. V. O. Kostroun, Nucl. Instr. and Meth. B10/11, 771 (1985).

58. E. D. Donets and V. P. Ovsyannikov, Sov. Phys. JETP 53, 466 (1981).

59. V. M. Lunev, V. D. Ovcharenko and V. M. Khoroshikh, Sov. Phys. Tech. Phys. 22(7), 855 (1977).

60. S. Goldsmith and R. L. Boxman, J. Appl. Phys. 51, 3649 (1980).

61. R. L. Boxman, S. Goldsmith, I. Izraeli and S. Shalev, IEEE Trans. Plasma Sci. PS-11, 138 (1983).

62. V. A. Ivanov, B. Juettner and H. Pursch, IEEE Trans. Plasma Sci. PS-13, 334 (1985).

63. Y. Jongen, Louvain-la-Neuve, Belgium, Report LC-8001 (1980).

64. H. I. West, Jr., Lawrence Livermore Laboratory Report UCRL-53391 (1982).

TABLE I

Charge state fractions and arc voltages measured for the cathode materials investigated here. The charge state fractions have been expressed both as electrical current and as particle current; mean charge states are also listed.

Element	Electrical current fractions (%)						Particle current fractions (%)						V_{arc}
	Q = 1	2	3	4	5	$\overline{Q}_e$	Q = 1	2	3	4	5	$\overline{Q}_p$	
C	100					1	100					1	
Mg	23	77				1.77	37	63				1.63	16
Al	38	52	10			1.72	56	39	5			1.48	20.5
Si	38	58	4			1.66	56	42	2			1.46	
Ti	3	80	17			2.14	6	82	12			2.05	20.5
Cr	14	73	13			1.99	25	67	8			1.82	20
Fe	18	74	8			1.90	31	64	5			1.73	20.5
Co	30	62	8			1.78	47	49	4			1.57	20.5
Ni	35	58	7			1.72	53	44	3			1.51	20
Cu	26	49	25			1.99	44	42	14			1.70	20.5
Zn	76	24				1.24	86	14				1.14	14
Zr	4	47	38	11		2.56	9	55	30	6		2.33	22
Nb	2	36	43	19		2.79	5	46	37	12		2.56	25.5
Mo	6	40	36	18		2.66	14	47	28	11		2.35	24.5
Rh	28	52	18	2		1.94	46	43	10	1		1.65	24
Pd	24	69	7			1.83	39	57	4			1.64	18
Ag	18	66	16			1.98	32	59	9			1.77	19
In	79	21				1.21	88	12				1.12	14
Sn	36	64				1.64	53	47				1.47	14
Gd	3	78	19			2.16	6	81	13			2.07	16.5
Ho	8	79	13			2.05	15	76	9			1.93	18
Ta	5	30	33	28	4	2.96	3	39	28	18	2	2.58	24.5
W	3	25	39	27	6	3.08	8	34	36	19	3	2.74	28
Pt	52	44	4			1.52	69	29	2			1.33	20.5
Au	28	69	3			1.75	44	54	2			1.58	18
Pb	47	53				1.53	64	36				1.36	12.5
Th	1	1	72	17		3.05	3	15	70	12		2.92	16
U	1	29	62	8		2.77	3	38	54	5		2.62	19

TABLE II

Comparison of charge state distributions measured in the present work with those obtained by other authors. I_{el}, I_{part} indicate that the charge state fractions are expressed in terms of electrical current or particle current, (see text for discussion on this point). Arc current: This work 200A; Ref 5 mostly 100A; Ref 6 100A except Ta 140A; Ref 8 100A except Mo 170A.

Element	Author	Charge State Fraction (%)				
		Q = 1	2	3	4	5
C	This work (I_{el})	100				
	" (I_{part})	100				
	Ref 6	96	4			
Mg	This work (I_{el})	23	77			
	" (I_{part})	37	63			
	Ref 5	50	50			
Al	This work (I_{el})	38	52	10		
	" (I_{part})	56	39	15		
	Ref 5	60	38	2		
	Ref 6	49	44	7		
Ti	This work (I_{el})	3	80	17		
	" (I_{part})	6	82	12		
	Ref 8	27	67	6		
Cr	This work (I_{el})	14	73	13		
	" (I_{part})	25	67	8		
	Ref 8	16	68	14	2	
Fe	This work (I_{el})	18	74	8		
	" (I_{part})	31	64	5		
	Ref 8	54	46			
Ni	This work (I_{el})	35	58	7		
	" (I_{part})	53	44	3		
	Ref 5	65	33	2		
	Ref 6	48	48	3		
Cu	This work (I_{el})	26	49	25		
	" (I_{part})	44	42	14		
	Ref 6	30	54	15		
	Ref 8	38	55	7		

Element	Author	$Q =$ 1	2	3	4	5
		Charge State Fraction (%)				
Zr	This work (I_{el})	4	47	38	11	
	" (I_{part})	9	55	30	6	
	Ref 6	14	60	21	5	
Mo	This work (I_{el})	6	40	36	18	
	" (I_{part})	14	47	28	11	
	Ref 6	16	69	13	2	
	Ref 8	3	33	42	19	3
Ag	This work (I_{el})	18	66	16		
	" (I_{part})	32	59	9		
	Ref 6	65	34	1		
Ta	This work (I_{el})	5	30	33	28	4
	" (I_{part})	13	39	28	18	2
	Ref 6	13	35	28	13	10

TABLE III

Comparison of arc voltages measured in the present work with those obtained by other workers.

Arc current: This work 200A; Ref 5 approx 200A except Pb 20A;

Ref 6 100A except Ta 140A; Ref 7 100A except Cu 80A, Fe and Mo 200A, W 250A;

Ref 8 100A except Mo 170A; Ref 9 100A-200A.

Material	Arc Voltage (V)					
	This work	Ref 5	Ref 6	Ref 7	Ref 8	Ref 9
Mg	16	15				12
Al	20.5	20.5	20			18
Ti	20.5			20	20	
Cr	20			18	19.5	
Fe	20.5			20	19	
Co	20.5					
Ni	20	19	18.5			
Cu	20.5	19.5	20.5	20	22	19.5
Zn	14	12		13		10
Zr	22		21.5			
Nb	25.5					
Mo	24.5		25.5	28	28	
Rh	24					
Pd	18					
Ag	19	17	16.5	20		
In	14					
Sn	14					12.5
Gd	16.5					
Ho	18					
Ta	24.5		24			
W	28					
Pt	20.5					
Au	18					
Pb	12.5	10.3				
Th	16					
U	19					

Extractor grids
Anode
Trigger Electrode
Pyrex vacuum chamber

Coolant flow

Cathode

Quartz sheath

Magnetic field coil

|← — — — 10 cm — — — — —→|
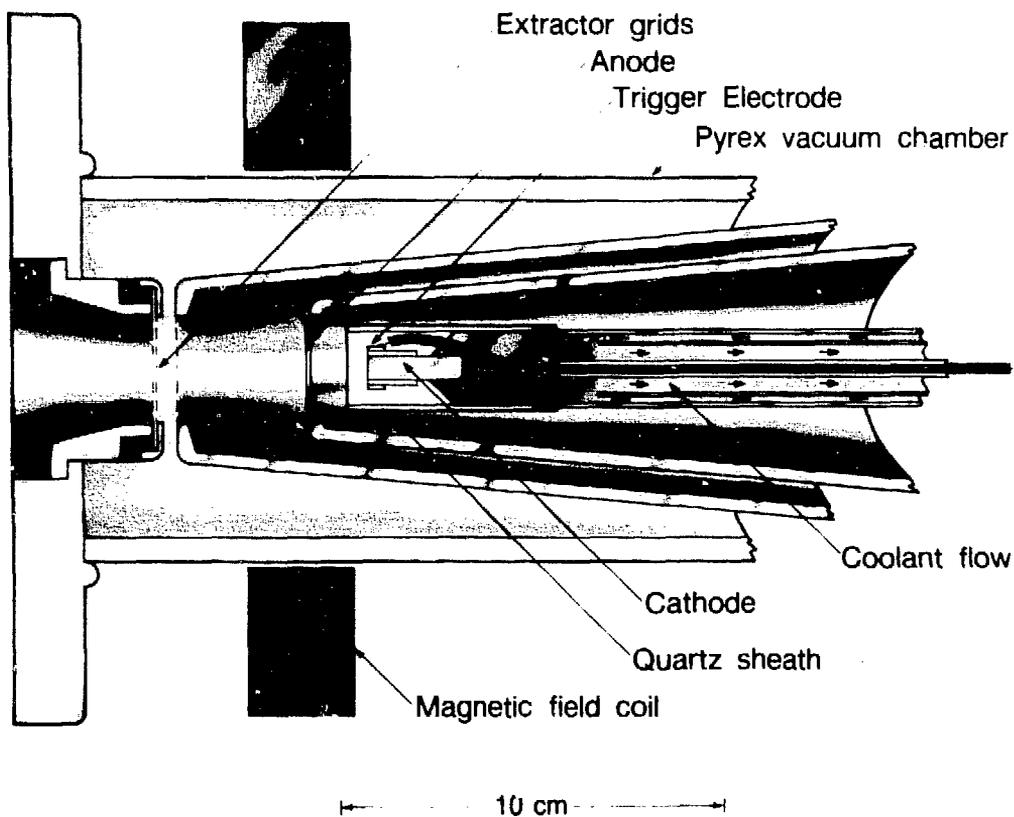
CBB 862-1362A

Fig. 1   Schematic of the ion source (MEVVA II).
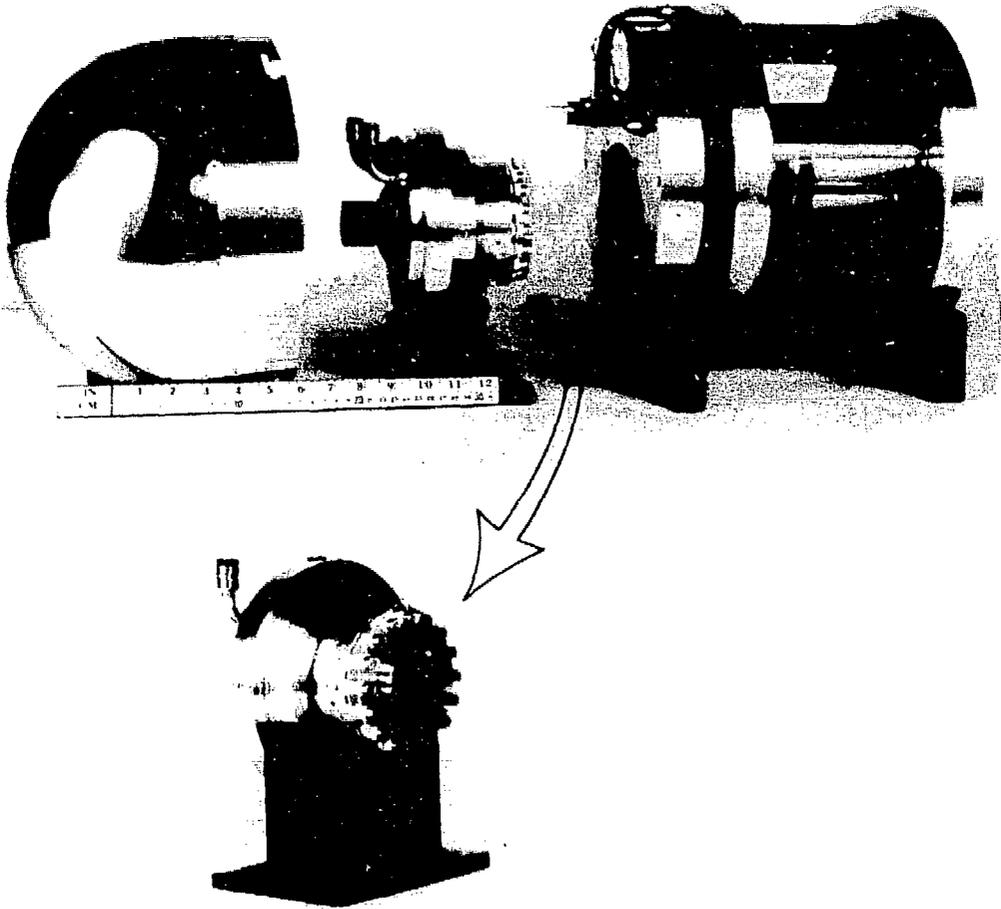
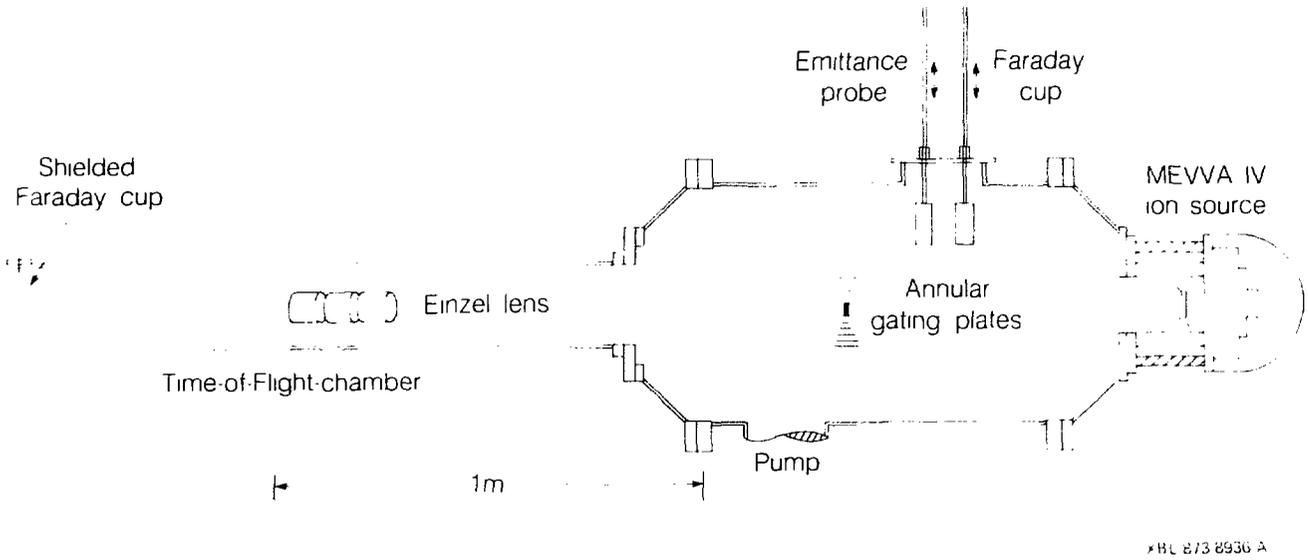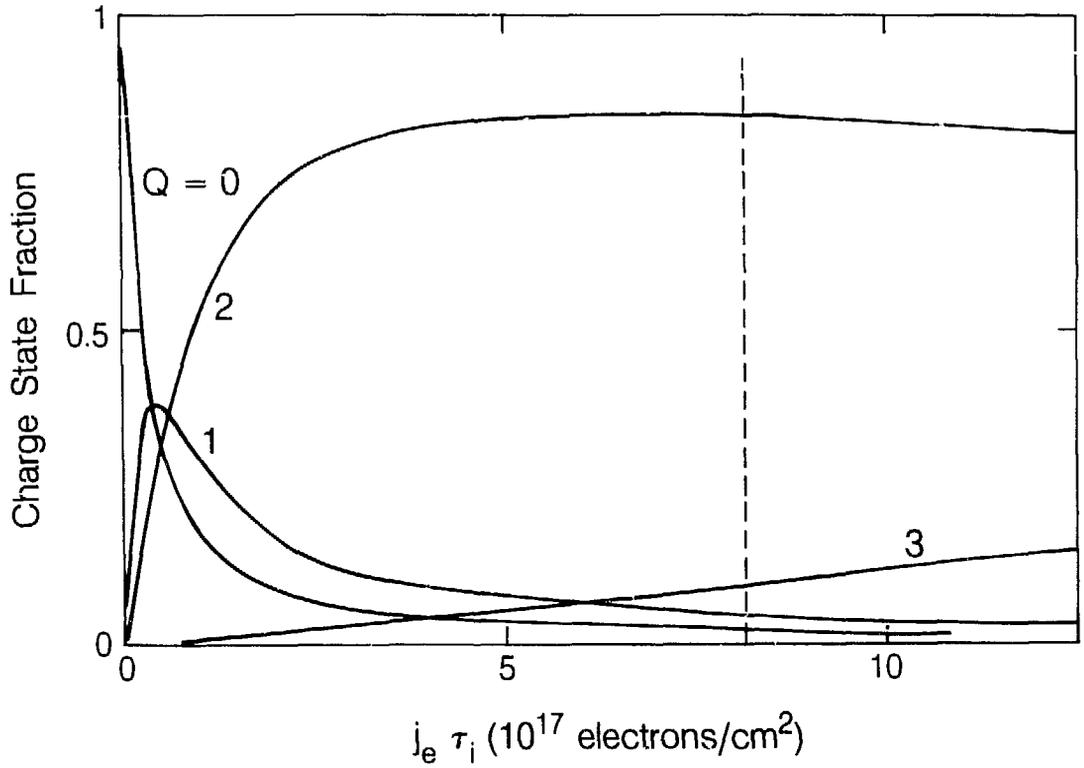Fig. 2   The MEVVA IV ion source, showing the multiple cathode configuration.

Shielded
Faraday cup

Emittance
probe

Faraday
cup

MEVVA IV
ion source

Einzel lens

Annular
gating plates

Time-of-Flight-chamber

Pump

1m

XBL 873 8936 A

Fig. 3 Schematic of the experimental configuration.

Fig. 4 Charge state distribution predicted by the stepwise ionization model. Titanium plasma, Maxwellian electron velocity distribution with T_e = 4.6 eV.

XBB 875-5170
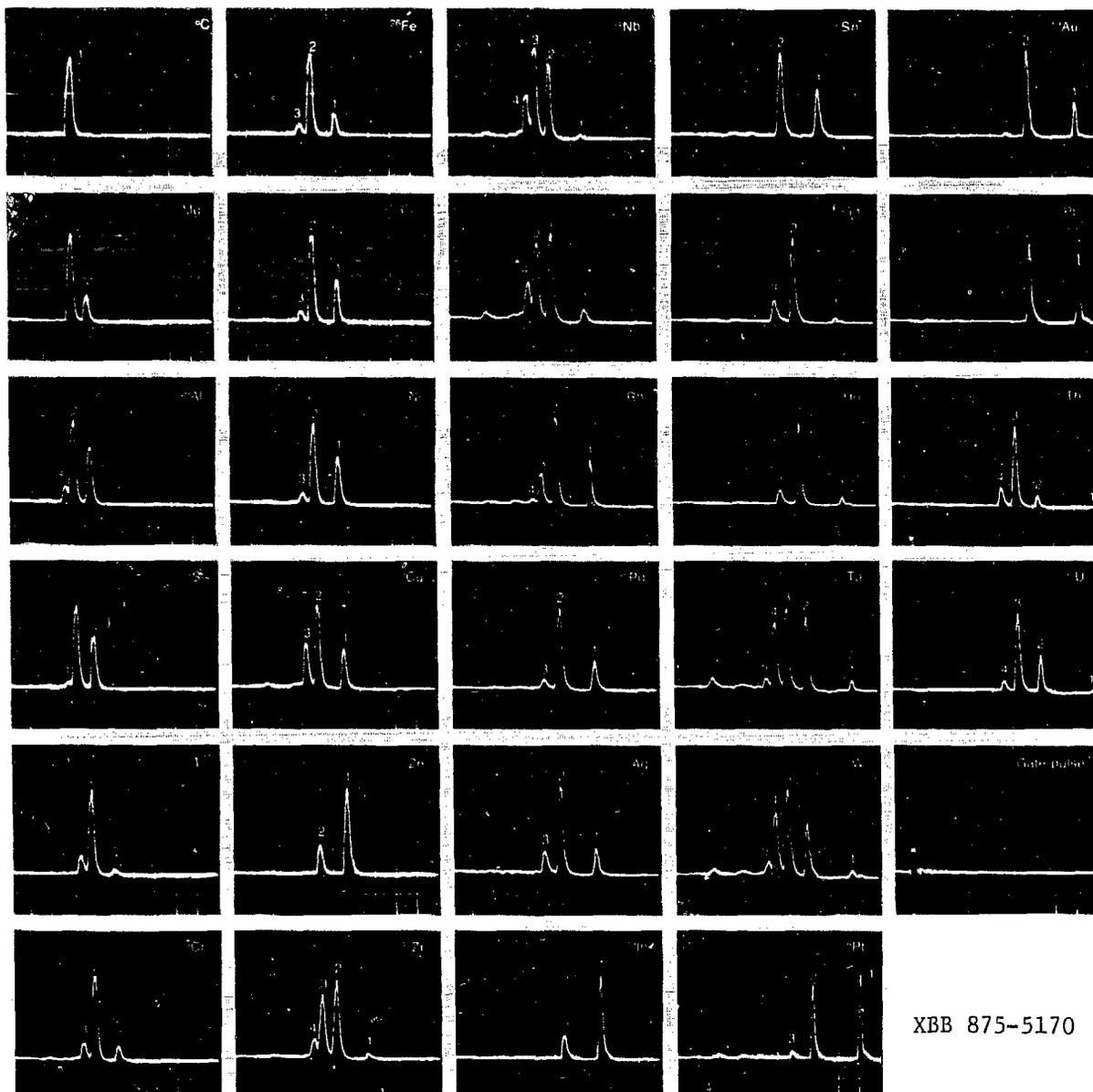
Fig. 5 Time-of-flight spectra for the range of elemental cathode materials investigated in this work. Vertical scale: current collected by the Faraday cup, gain approx. 100 μA/cm. Sweep speed: 1 μs/cm.

Gate Pulse   Q: 2 1 3 2   1

C   Ti
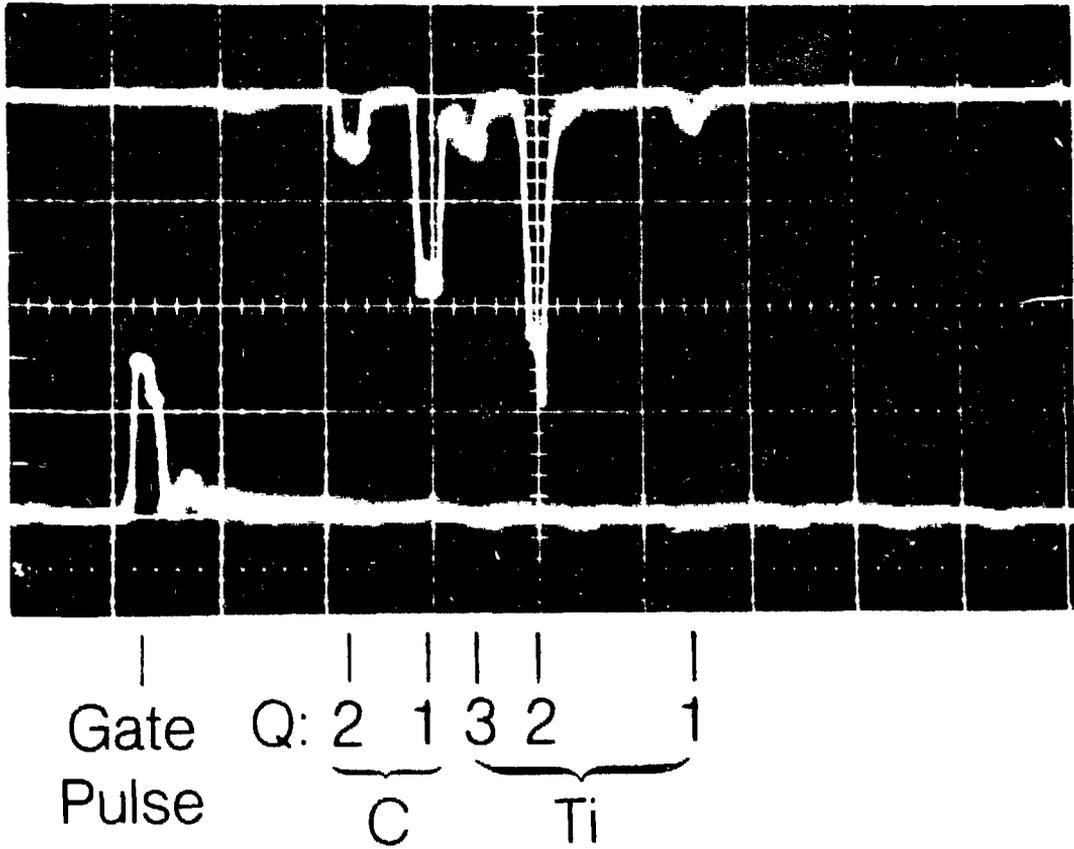
XBB 868-6234

Fig. 6 (a) Time-of-flight spectrum for titanium carbide.

Gate   S⁺   Pb²⁺   Pb⁺
Pulse
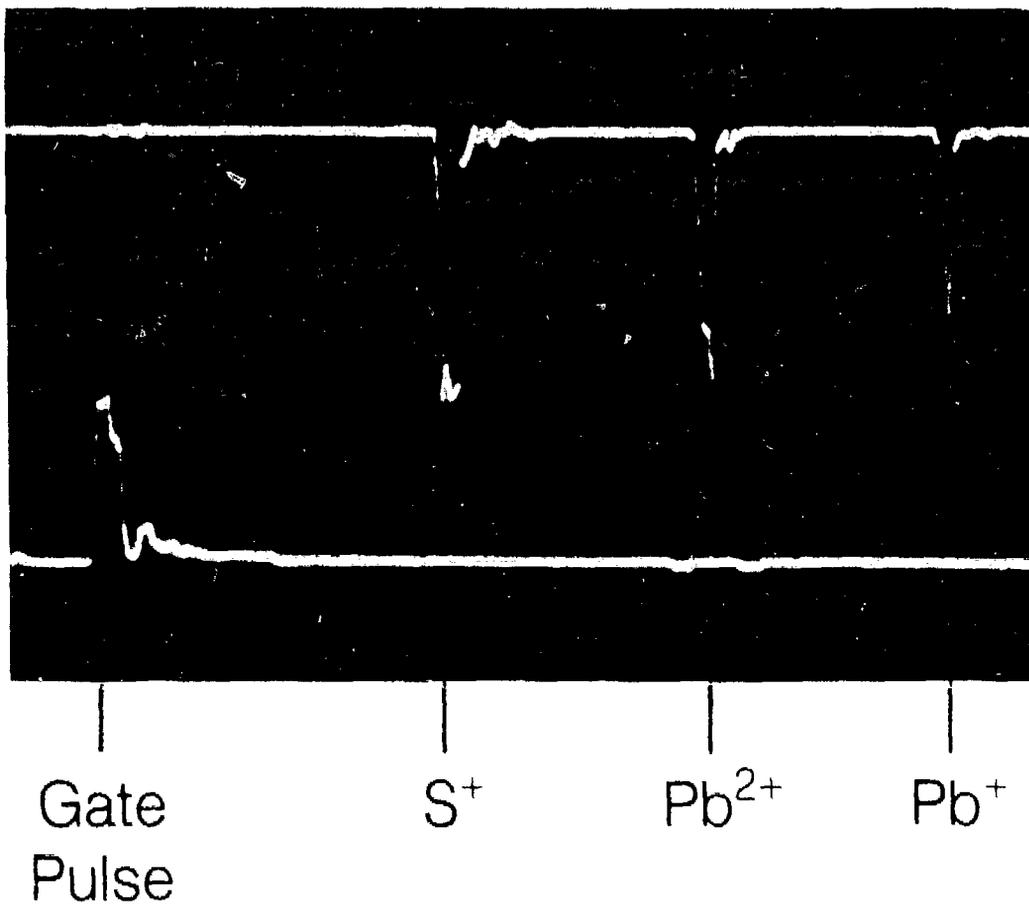
XBB 865-3967

Fig. 6 (b) Time-of-flight spectrum for lead sulfide.
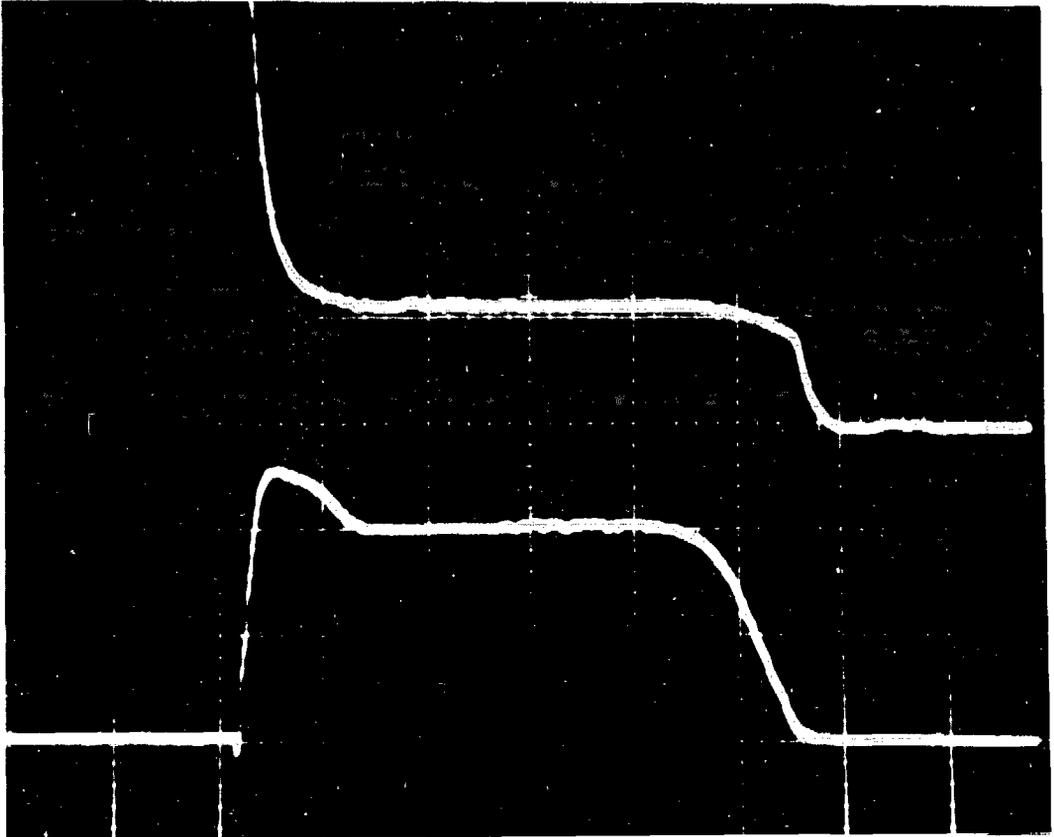
Fig. 7   Arc voltage (upper trace, 20 V/cm), and arc current (lower trace, 100 A/cm), for the case of a copper cathode.   Sweep speed is 50 μs/cm. (Note that the voltage trace is initially off-scale until conduction starts).
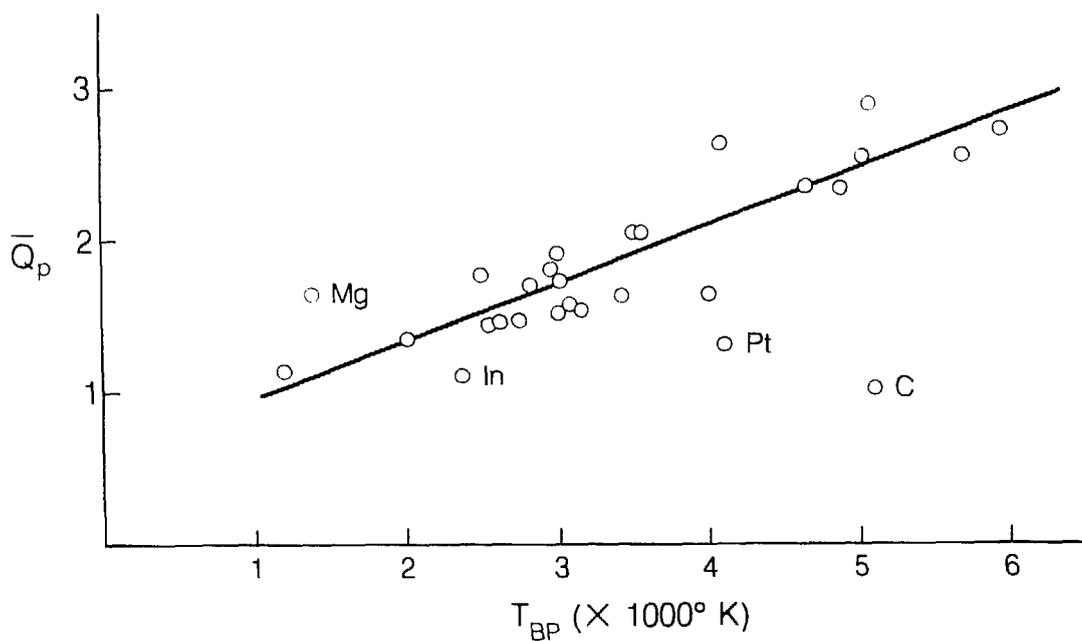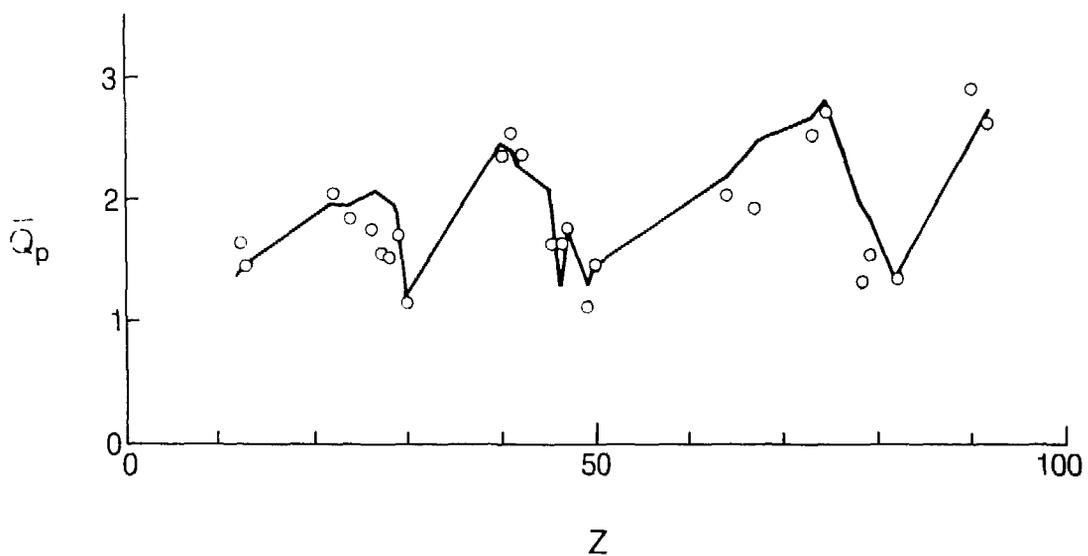
Fig. 8 Measured mean charge state, $\bar{Q}_p$, as a function of the Boiling Point
temperature (°K) of the cathode material. The straight line is the
best fit to the data points (except C, Mg, In, Pt) and is given by $\bar{Q}_p$
= $0.38(T_{BP}/1000) + 0.6$.
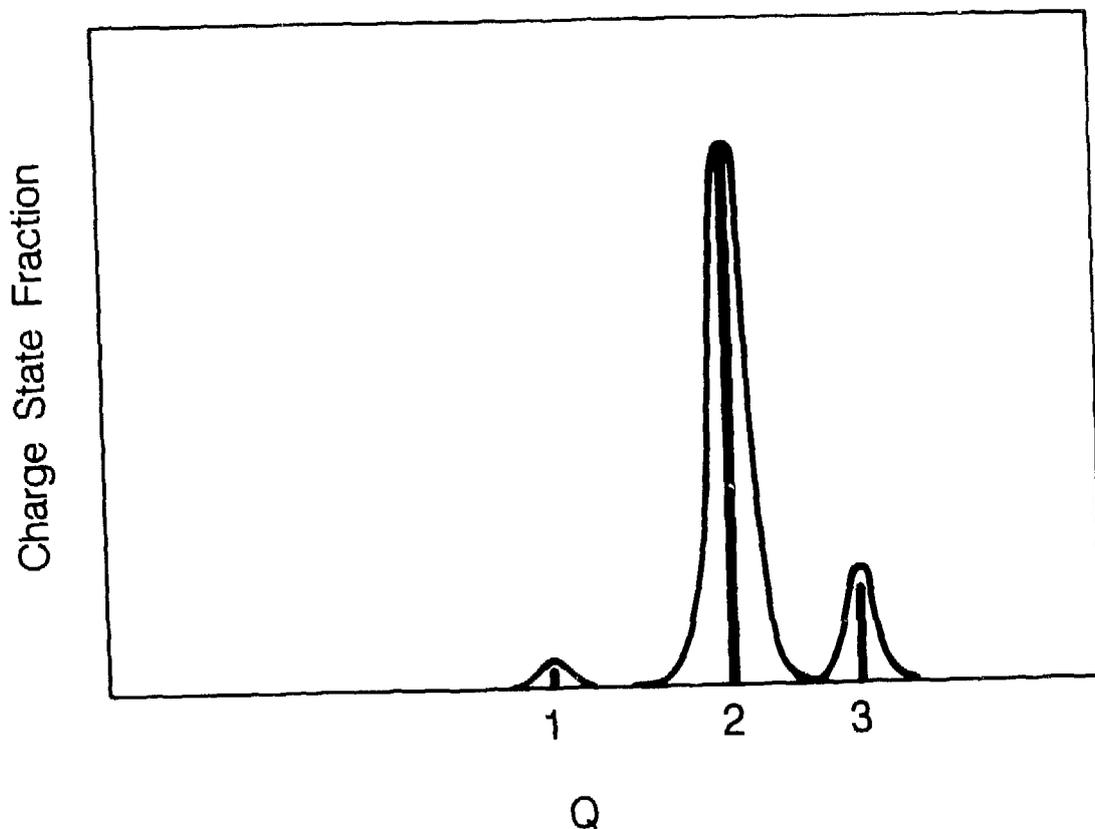
XBL 879-9787

Fig. 9 Measured and calculated charge state distributions for titanium. The
experimental CSD has been taken from Fig. 5; the theoretical CSD,
indicated by the vertical lines, has been taken from Fig. 4 at the
time indicated. Electrical current is shown, so the Fig. 4 fractions
have been multiplied by Q, $I_e = QI_p$.

Fig. 10 Measured mean charge state, $\bar{Q}_p$, as a function of atomic number Z. The line indicates the mean charge state predicted by the theory presented here; see text for discussion of input parameters.

XBL 879-9786